Mutations in the MicroRNA Complementarity Site of the *INCURVATA4* Gene Perturb Meristem Function and Adaxialize Lateral Organs in Arabidopsis[1][W]

Isabel Ochando[2], Sara Jover-Gil[2,3], Juan José Ripoll, Héctor Candela[4], Antonio Vera, María Rosa Ponce, Antonio Martínez-Laborda, and José Luis Micol*

División de Genética, Universidad Miguel Hernández, Campus de San Juan, 03550 Alicante, Spain (I.O., J.J.R., A.V., A.M.-L.); and División de Genética and Instituto de Bioingeniería, Universidad Miguel Hernández, Campus de Elche, 03202 Elche, Alicante, Spain (S.J.-G., H.C., M.R.P., J.L.M.)

Here, we describe how the semidominant, gain-of-function *icu4-1* and *icu4-2* alleles of the *INCURVATA4* (*ICU4*) gene alter leaf phyllotaxis and cell organization in the root apical meristem, reduce root length, and cause xylem overgrowth in the stem. The *ICU4* gene was positionally cloned and found to encode the ATHB15 transcription factor, a class III homeodomain/leucine zipper family member, recently named CORONA. The *icu4-1* and *icu4-2* alleles bear the same point mutation that affects the microRNA complementarity site of *ICU4* and is identical to those of several semidominant alleles of the class III homeodomain/leucine zipper family members *PHABULOSA* and *PHAVOLUTA*. The *icu4-1* and *icu4-2* mutations significantly increase leaf transcript levels of the *ICU4* gene. The null *hst-1* allele of the *HASTY* gene, which encodes a nucleocytoplasmic transporter, synergistically interacts with *icu4-1*, the double mutant displaying partial adaxialization of rosette leaves and carpels. Our results suggest that the *ICU4* gene has an adaxializing function and that it is down-regulated by microRNAs that require the HASTY protein for their biogenesis.

MicroRNAs (miRNAs) are small regulatory RNAs present in organisms as diverse as plants and humans. In plants, most of the miRNAs studied guide cleavage of their mRNA targets after miRNA-mRNA pairing. In Arabidopsis (*Arabidopsis thaliana*), miRNAs perfectly or almost perfectly match their mRNA targets, which prompted several authors to perform computational analyses to predict miRNA targets. Many putative miRNA target genes found in this way encode transcription factors that control specific aspects of plant development (for review, see Bartel and Bartel, 2003; Bartel, 2004; Bartel and Chen, 2004; Baulcombe, 2004; Dugas and Bartel, 2004; Chen, 2005; Du and Zamore, 2005; Jover-Gil et al., 2005; Kim, 2005).

Class III homeodomain/Leu zipper (HD-Zip III) genes share a conserved miRNA complementarity site, which is cleaved after miRNA-mRNA pairing (for review, see Bowman, 2004). Three well-known HD-Zip III family members are *PHABULOSA* (*PHB*; McConnell and Barton, 1998), *PHAVOLUTA* (*PHV*; McConnell et al., 2001), and *REVOLUTA* (*REV*, also known as *IFL1* and *AVB1*; Alvarez, 1994; Zhong and Ye, 1999; Zhong et al., 1999). The expression of *PHB*, *PHV*, and *REV* is generalized in the incipient leaves, but becomes restricted to the adaxial domain after primordium emergence (Eshed et al., 2001; McConnell et al., 2001; Emery et al., 2003; Heisler et al., 2005). The absence of PHB, PHV, and REV from the abaxial domain of early leaves allows expression of the KANADI (KAN; Eshed et al., 1999; Kerstetter et al., 2001) and YABBY (YAB; Siegfried et al., 1999; Kumaran et al., 2002; Emery et al., 2003) abaxializing proteins. These recent studies extended classical surgical experiments (Sussex, 1954) and provided evidence that certain genes are required in lateral organs to specify the identities of their adaxial and abaxial domains.

HASTY (*HST*) is the Arabidopsis ortholog of the genes encoding mammalian exportin 5 and MSN5 of yeast (*Saccharomyces cerevisiae*), two importin β-like receptors (Telfer and Poethig, 1998; Bollman et al., 2003). Because human exportin 5 exports miRNA precursors from the nucleus to the cytoplasm (Gwizdek et al., 2003; Yi et al., 2003; Bohnsack et al., 2004), a similar role has been proposed for HST (Hunter and Poethig, 2003)

[1] This work was supported by the Ministerio de Educación y Ciencia of Spain (research grants BMC2002–02840 and BFU2005–01031 to J.L.M., BIO2002–04083–C03–03 to A.M.L., and BMC2003–09763 to M.R.P.). S.J.-G. and I.O. were fellows of the Ministerio de Educación y Ciencia of Spain and the Generalitat Valenciana, respectively.

[2] These authors contributed equally to the paper.

[3] Present address: Lawrence Berkeley National Laboratory, University of California, Berkeley, CA 94720.

[4] Present address: Plant Gene Expression Center, University of California, Albany, CA 94710.

* Corresponding author; e-mail jlmicol@umh.es; fax 34–96–665–8511.

The author responsible for distribution of materials integral to the findings presented in this article in accordance with the policy described in the Instructions for Authors (www.plantphysiol.org) is: José Luis Micol (jlmicol@umh.es).

[W] The online version of this article contains Web-only data.

Article, publication date, and citation information can be found at www.plantphysiol.org/cgi/doi/10.1104/pp.106.077149.

based on its localization at the nuclear periphery and the phenotypic effects of *hst* alleles, which are reminiscent of those caused by mutations in genes of the miRNA pathway. However, the demonstration that miR159 precursors are cleaved within the nucleus (Papp et al., 2003) suggested that HST might instead export mature miRNAs to the cytoplasm. Furthermore, although loss of function of *HST* causes a generalized reduction of miRNA levels, it does not cause miRNAs to accumulate in the nucleus (Park et al., 2005).

In an attempt to identify genes required for leaf morphogenesis, we searched for Arabidopsis leaf mutants (Berná et al., 1999; Serrano-Cartagena et al., 1999), some of which displayed involute leaves, a phenotype that we named Incurvata (Icu). Two of these mutants, *icu4-1* and *icu4-2*, previously isolated by G. Röbbelen (Bürger, 1971; Kranz, 1978), were found to be allelic and semidominant and to synergistically interact with *hst* alleles (Serrano-Cartagena et al., 2000). Here, we describe the positional cloning of the *ICU4* gene, which encodes the HD-Zip III transcription factor ATHB15, also named CORONA (CNA; Green et al., 2005; Prigge et al., 2005). Our results suggest that the *ICU4* gene is down-regulated by miRNAs that require the HST protein for their biogenesis and that it encodes a protein with adaxializing activity.

RESULTS

Positional Cloning of the *ICU4* Gene

We followed a map-based strategy for cloning the *ICU4* gene, which we previously mapped to chromosome 1 between the T27K12-Sp6 and nga128 microsatellite markers (Serrano-Cartagena et al., 2000). The genotyping of 130 *icu4-1* homozygotes selected from an F_2 mapping population derived from a Columbia-0 (Col-0) $\times$ *icu4-1/icu4-1* cross allowed us to narrow down the candidate region to five overlapping bacterial artificial chromosome clones (Fig. 1A). One such bacterial artificial chromosome, F5F19, contained the At1g52150 gene, a member of the HD-Zip III family also known as *CNA* and *ATHB15*. Because semidominant alleles of other genes of this family perturb leaf morphology, we sequenced the gene in the *icu4-1* and *icu4-2* mutants. Both alleles were found to carry the same point mutation, a G-to-A transition, in the fifth position of exon 5, within a complementarity site for the miR165 and miR166 miRNAs (Fig. 1, A and B). This mutation is predicted to cause a Gly-to-Asp amino acid change within the steroidogenic acute regulatory-related lipid transfer (START; Ponting and Aravind, 1999) domain, which is highly conserved in HD-Zip III family members of Arabidopsis and maize (*Zea mays*; Fig. 1, B and C; McConnell et al., 2001; Rhoades et al., 2002; Juarez et al., 2004). The mutation found in *icu4-1* and *icu4-2* is identical to those of semidominant alleles of the *PHB* and *PHV* genes (Fig. 1B; McConnell et al., 2001) and different from those of semidominant alleles of the *REV* gene of Arabidopsis and *rolled leaf1* (*rld1*) of maize. All these mutations impair pairing of miR165/166 and their targets (Emery et al., 2003; Juarez et al., 2004; Zhong and Ye, 2004; Fig. 1B). We did not find additional mutations in the *icu4-1* and *icu4-2* mutants compared to their wild-type ancestor Enkheim-2 (En-2) after sequencing all the exons and introns of the At1g52150 gene and several hundred base pair upstream of the initiation codon and downstream of the stop codon. Given that there is little information on their isolation by Röbbelen, we cannot rule out that *icu4-1* and *icu4-2* represent two independent isolations of a single mutation.

As indicated in http://www.ncbi.nlm.nih.gov/UniGene, the At1g52150 gene is 4,968 bp long and includes 18 exons. Its transcriptional activity is supported by six full-length Col-0 cDNA sequences deposited in databases. Its predicted protein product contains the three domains characteristic of HD-Zip III family members (Schrick et al., 2004; Fig. 1C): a homeodomain (HOX; residues 17–77), a basic region Leu zipper (bZIP) domain (69–115), and a START lipid-binding domain (152–366). Comparison of the At1g52150 sequence in several wild-type lines revealed a high degree of polymorphism. We found that residues in positions 181, 238, 622, and 629 are Val, Glu, Gln, and Ala, respectively, in Col-0, but Ile, Asp, Leu, and Thr in En-2 and ecotype Landsberg *erecta* (L*er*). Residue 641 was Ile in Col-0 and L*er*, but Thr in En-2. Of these, only the Val residue at position 181 was conserved among the members of the HD-Zip III family.

Functional Nature of *icu4* Mutations

The most conspicuous phenotypic trait of the *icu4-1* and *icu4-2* mutants is rosette leaf incurvature (i.e. the lamina curls upward; Fig. 2, A–C and E–G; Serrano-Cartagena et al., 1999, 2000). Leaf incurvature in *ICU4/icu4-1* heterozygotes (Fig. 2, C and G) was weaker than in *icu4-1/icu4-1* homozygotes (Fig. 2, B and F), but still clearly distinguishable from the wild type (Fig. 2, A and E), particularly at early stages of leaf expansion (Fig. 2G). The expressivity of the leaf phenotype was variable in *ICU4/icu4-1* heterozygotes, ranging from slightly affected plants with only the first two leaves incurved, to plants having all the rosette leaves with incurved margins and an irregular lamina surface (Fig. 2C).

We performed a dosage analysis to ascertain whether the semidominance of the *icu4-1* allele results from a gain-of-function mutation or, alternatively, from a loss-of-function mutation at a haploinsufficient locus. To this end, we crossed the tetraploid line CS3151 to *icu4-1/icu4-1* plants and studied the phenotype of the resulting triploid F_1 progeny. Incurvature was observed in the expanding leaves of *ICU4/ICU4/icu4-1* triploids (Fig. 2, D and H) similar to that displayed by *ICU4/icu4-1* diploid plants (Fig. 2, C and G). The leaves of the triploid progeny of CS3151 $\times$ En-2 control crosses were not incurved, confirming that the phenotype of *ICU4/ICU4/icu4-1* was an effect of a gain of function in the *icu4-1* allele.

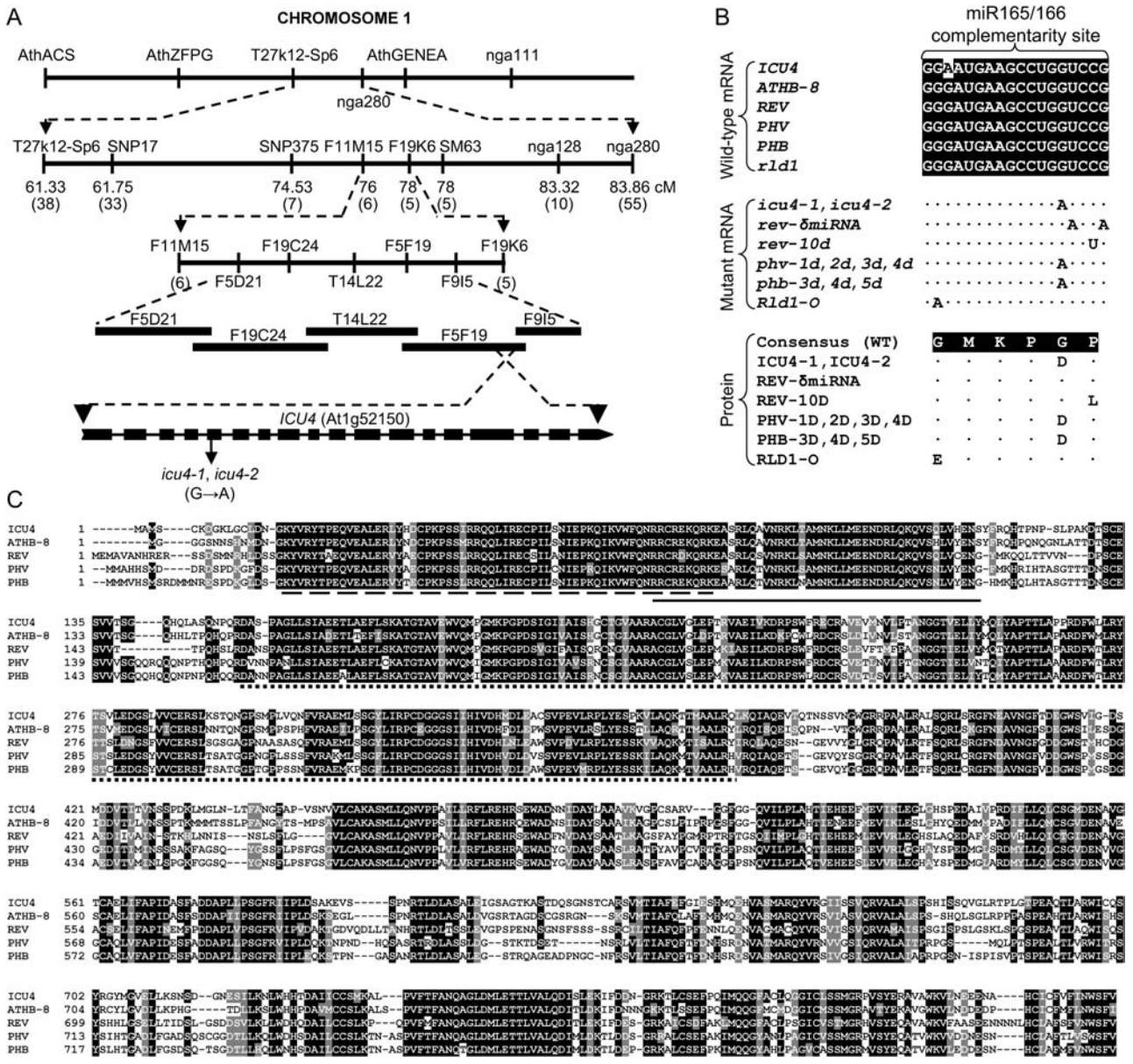

Figure 1. Cloning and structural analysis of the *ICU4* gene. A, Map-based cloning of the *ICU4* gene, with indication (in parentheses) of the number of informative recombinants found relative to each of the markers used for linkage analysis. B, Complementarity site for the miR165 and miR166 miRNAs in the mRNA of the *rld1* gene of maize and those of HD-Zip III family genes of Arabidopsis. The effects of some gain-of-function mutations disrupting the miR165/166 complementarity site is shown for both mRNA and protein sequences (McConnell et al., 2001; Emery et al., 2003; Juarez et al., 2004; this work). The *amphivasal vascular bundle 1* (*avb1*; Zhong and Ye, 2004) mutation is identical to *rev-10d*. C, Alignment of HD-Zip III family proteins in a Col-0 background. The dashed, continuous, and dotted lines indicate the HOX, bZIP, and START domains, respectively. Identical and similar residues are colored in black and gray, respectively.

In addition, an RNA interference (RNAi) construct for the At1g52150 gene (35S::*ICU4*-RNAi) was transferred to *icu4-1/icu4-1* plants. Six primary transformants for the 35S::*ICU4*-RNAi construct displayed flattened leaves similar to those of the wild type, a phenotypic trait that cosegregated with the construct in the T_2 and subsequent generations (Fig. 2I), which is consistent with the hypothesis that *icu4-1* and *icu4-2* are gain-of-function mutations. The ability of the transgene to suppress the mutant phenotype further supports the idea that the *icu4* mutations affect the expression of the At1g52150 gene. En-2 plants transformed with the 35S::*ICU4*-RNAi construct did not show any mutant phenotypic trait.

We searched for insertional, putatively null alleles of *ICU4* in public collections (see "Materials and

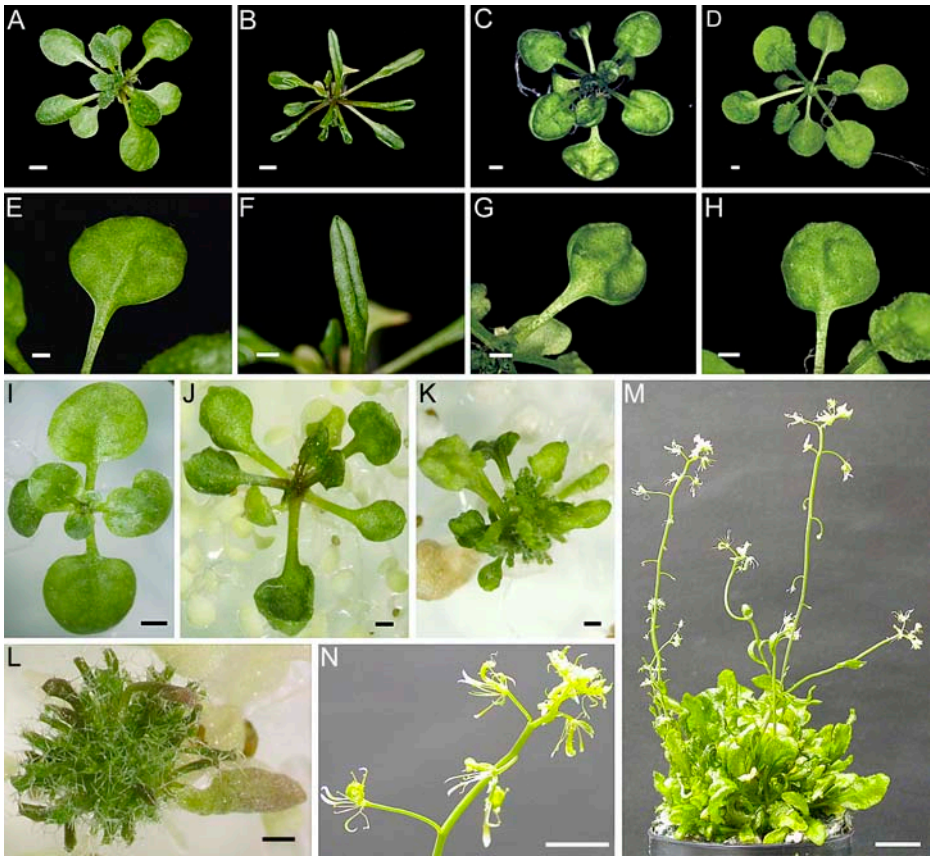

Figure 2. Some phenotypic traits of the *icu4* mutants and transgenic plants obtained in this work. Rosettes and leaves are shown from the En-2 wild type (A and E), an *icu4-1*/*icu4-1* homozygote (B and F), an *ICU4*/*icu4-1* heterozygote (C and G), and an *ICU4*/*ICU4*/*icu4-1* triploid (D and H), the latter showing traits similar to those displayed by the *ICU4*/*icu4-1* heterozygote. I, Transgenic plant harboring, in an *icu4-1*/*icu4-1* background, the RNAi construct (35S::*ICU4*-RNAi), whose leaves are flattened like those of the wild type. J to N, Transgenic plants harboring, in an En-2 background, the 35S::*ICU4*-G189D transgene, which carries the *icu4-1* mutation. Examples are shown of weak (J), intermediate (K, M, and N), and strong (L) degrees of morphological aberrations caused by the 35S::*ICU4*-G189D transgene, which include radialized leaves (L) and partially radialized floral organs (M and N). Scale bars indicate 2 mm (A and B), 1 mm (C–E and G–L), 500 μm (F), 1 cm (M), and 0.5 cm (N). Pictures were taken 21 (A–H), 14 (I), 20 (J), 28 (K), 35 (L), and 90 (M and N) d after sowing.

Methods'') and found two, *icu4-3* and *icu4-4*, which did not cause any mutant phenotype in homozygosis, neither on their own nor in double-mutant combinations with null alleles of the *ATHB8* gene (data not shown). This result is also in close agreement with the behavior of our RNAi construct, as well as with the lack of a discernible phenotype recently found in homozygotes for the null *cna-2* allele (Prigge et al., 2005). Our results and those of Prigge et al. (2005) are in striking contrast with those of Kim et al. (2005), who recently reported severe phenotypic alterations in transgenic plants bearing an antisense *ATHB15* construct.

To further analyze the involvement of At1g52150 on the phenotype of *icu4* mutants, the cDNAs of the wild-type *ICU4* and mutant *icu4-1* (*ICU4*-G189D) alleles were fused to the constitutive cauliflower mosaic virus 35S promoter and transferred to the En-2 wild type. All transgenic plants overexpressing the wild-type *ICU4* cDNA were late flowering but displayed almost normal leaf morphology (data not shown). In contrast, we identified two classes of transgenic plants overexpressing the *icu4-1* mutant cDNA, one of them including five phenotypically wild-type lines that might result from the silencing of the transgene. The remaining 12 35S::*ICU4*-G189D transformants were late flowering or did not flower at all, and exhibited a wide spectrum of mutant phenotypes, ranging from four lines with moderately incurved leaves (Fig. 2J) to more severely affected plants, showing radialized leaves (Fig. 2L) or an intermediate phenotype with radialized and trumpet-shaped leaves (Fig. 2K), which were apparently adaxialized. The most affected transformants (Fig. 2L, three primary transformants) never flowered. Five primary transformants with an intermediate phenotype also displayed partially radialized floral organs (Fig. 2, M and N) and abnormal pistils, resulting in sterility.

The four 35S::*ICU4*-G189D lines with moderate phenotype were very similar to the *icu4-1* mutant and the *mATHB15* transgenic plants (Kim et al., 2005), which overexpress a construct carrying silent mutations in its miRNA complementarity site. The very strong phenotypes of some of our 35S::*ICU4*-G189D transgenics are likely to be due to the 5′- and 3′-untranslated sequences, which might cause expression of the transgene at high levels and were not completely incorporated into *mATHB15* (Kim et al., 2005).

The Morphological Phenotype of *icu4* Mutants

The phenotype of *icu4-1* and *icu4-2* mutants was pleiotropic and more severe at 25°C than at 20°C or 18°C (data not shown), as described for semidominant *phb-1d* alleles (McConnell and Barton, 1998). Some *icu4-1* and *icu4-2* homozygotes, when grown at 25°C, displayed two inflorescences that bolted simultaneously

(data not shown), suggesting that the shoot apical meristem had split during the vegetative phase. The epidermis of *icu4-1/icu4-1* leaves contained smaller pavement cells and more stomata than the wild type, as observed on both sides of the leaves by scanning electron microscopy (Fig. 3, A–D). Finger-like outgrowths were occasionally observed on the abaxial surface of mutant leaves (data not shown). In addition, all trichomes found on the adaxial epidermis of *icu4-1/icu4-1* vegetative leaves had supernumerary branches (from four to six; Fig. 3E). Interestingly, the abaxial epidermis of all *icu4-1/icu4-1* vegetative leaves completely lacked trichomes. Mesophyll cell size was normal, as shown by confocal microscopy (data not shown). Most cauline leaves of *icu4-1* homozygotes were incurved, although in some cases its lamina curled down, whereas the margin and the apex curled up (Fig. 3, F and G).

The *ICU4* gene has previously been shown to be expressed in the vasculature, as seen in plants carrying a pATHB-15::β-glucuronidase (GUS) transgene (Ohashi-Ito and Fukuda, 2003). To test whether the gain-of-function *icu4-1* mutation altered the leaf venation pattern, we studied the expression of the pATHB-8-GUS reporter transgene, which is restricted to provascular cells and has previously been used to characterize the development of the vascular system in leaves and stems (Baima et al., 1995; Kang and Dengler, 2002; Kang et al., 2003). The pattern of GUS staining revealed no differences between the wild-type and *icu4-1/icu4-1* mutant plants (data not shown).

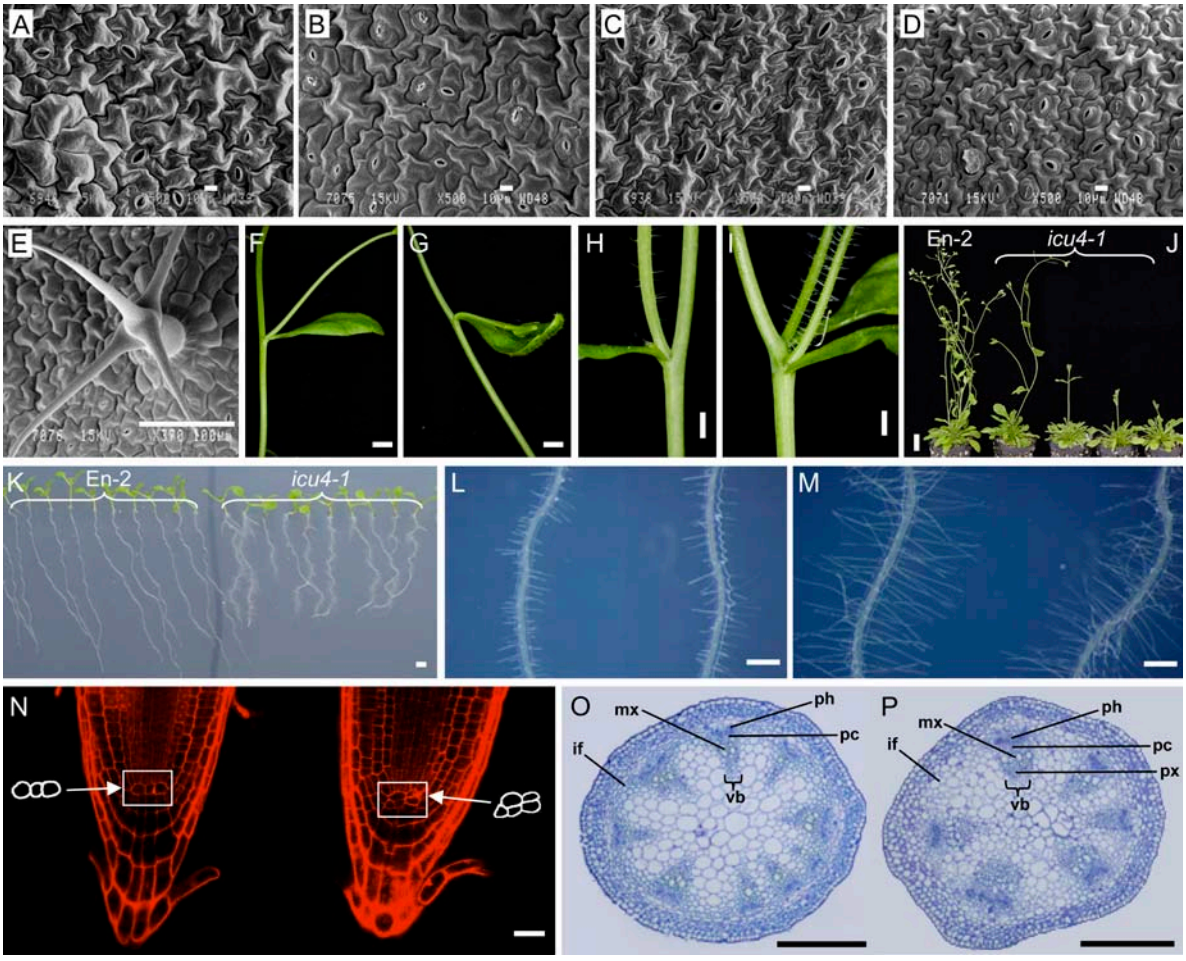

Figure 3. Some morphological and ultrastructural phenotypic traits of *icu4-1/icu4-1* homozygous plants. A to E, Scanning electron micrographs are shown of the adaxial (A and B) and the abaxial (C and D) epidermis of En-2 (A and C) and *icu4-1/icu4-1* (B and D) first leaves, and a four-branched *icu4-1/icu4-1* trichome (E). F and G, Wild-type En-2 (F) and incurved *icu4-1/icu4-1* cauline leaves (G). H and I, Cauline leaf and axillary shoot formation in En-2 (H) and *icu4-1/icu4-1* (I) plants. J, Different degrees of late flowering in *icu4-1/icu4-1* individuals. K to M, En-2 and *icu4-1/icu4-1* roots grown in vertically oriented plates (K), which are magnified (L and M), respectively. N to P, Confocal micrographs of propidium iodide-stained En-2 (left) and *icu4-1/icu4-1* (right) root tips (N), with a drawing of the founder and cortex initial cells. Transverse sections of wild-type (O) and *icu4-1/icu4-1* (P) stems. if, Interfascicular fibers; mx, metaxylem; pc, procambium; ph, phloem; px, protoxylem; vb, vascular bundle. Scale bars indicate 10 μm (A–D), 100 μm (E, O, and P), 1 cm (J), 2 mm (F, G, and K), 1 mm (H and I), 500 μm (L and M), and 20 μm (N). Pictures were taken 21 (A–E), 30 (F–I), 50 (J), 8 (K–M), and 5 (N) d after sowing.

The phyllotaxis was found to be altered in *icu4-1/icu4-1* rosettes. In the wild type, the divergence angle between the first and second rosette leaves is 180° and approaches 137.5° for the remaining leaves (Kang et al., 2003). In contrast, we observed a 180° angle until the fifth or sixth leaf in *icu4-1/icu4-1* rosettes (Fig. 2, B and C), extending the number of nodes with subdecussate phyllotaxis, which is characteristic of juvenile leaves. The frequent presence of two cauline leaves, with their associated axillary shoots, arising from a single node suggests that the allocation of cells to make cauline leaves is also altered in *icu4-1* (Fig. 3, H and I). Because phyllotactic defects are often associated with abnormal size or shape of the meristem, we compared *icu4-1/icu4-1* and wild-type meristems, finding no differences between them (Supplemental Fig. 1).

The *icu4-1* and *icu4-2* homozygotes were late flowering. Bolting was found to occur 24.9 ± 3.9 d after sowing in En-2 (n = 25 plants), but 39.3 ± 2.6 d after sowing in *icu4-1/icu4-1* plants (n = 35). Some of the latter bolted as late as 50 d after sowing (Fig. 3J). As expected, the delayed flowering was correlated with an increase in the number of rosette leaves, which was 14.9 ± 2.0 for En-2 (as determined 40 d after sowing) and 39.0 ± 7.7 for *icu4-1/icu4-1* (50 d after sowing).

The root system of *icu4-1/icu4-1* plants had longer root hairs and more secondary roots than the wild type (Fig. 3, K–M). In addition, *icu4-1/icu4-1* primary roots were 56.25% shorter than in the wild type, as determined 14 d after sowing. In agreement with this, we found a disorganized root apical meristem with extra cells within or next to the quiescent center of some *icu4-1/icu4-1* primary roots (Fig. 3N). The shoots of *icu4-1/icu4-1* plants usually had fewer, thicker, vascular bundles than the En-2 wild type. Transverse sections of *icu4-1/icu4-1* shoot vascular bundles showed enlarged metaxylem tracheids and extra layers of procambial cells located between overproliferated phloem and xylem cells, as well as a poor lignification of the interfascicular fibers (Fig. 3, O and P). Transverse sections of leaves, however, did not reveal obvious structural differences between the veins of *icu4-1/icu4-1* and wild-type plants (data not shown).

The *icu4 hst* Double Mutants

We previously described a synergistic interaction between the *icu4* and *hst* mutations based on the rosette phenotype of the *icu4-1 hst-5* double mutants (Serrano-Cartagena et al., 2000). We obtained an additional double mutant using *hst-1*, a null allele that had been thoroughly characterized by previous authors (Fig. 4A; Telfer and Poethig, 1998; Bollman et al., 2003). The *icu4-1/icu4-1; hst-1/hst-1* double-mutant plants showed variable expressivity because most of their vegetative leaves were helically rotated (Fig. 4B), and some of them were radialized and completely covered by trichomes (Fig. 4C), which suggests that they were partially adaxialized.

In addition, we characterized the phenotype of stage 12 and stage 14 gynoecia (Smyth et al., 1990; Ferrándiz et al., 1999) using optical and scanning electron microscopy. At stage 12, wild-type En-2 (Fig. 5A) and mutant *icu4-1/icu4-1* (Fig. 5B) pistils were indistinguishable, although after pollination *icu4-1/icu4-1* siliques were slightly smaller, probably due to a modest decrease of male fertility. On the other hand, most stage 12 *hst-1/hst-1* pistils were almost normal, although they were medially flattened and their stigmata (Fig. 5C) were larger than those of L*er*. Flowers appearing late in *hst-1/hst-1* inflorescences frequently had pistils that were unfused in the apical region, as previously described (Bollman et al., 2003). Transverse sections of En-2 and *icu4-1/icu4-1* fruits did not show any difference at stage 14 (Fig. 5D), whereas those of *hst-1/hst-1* showed an incompletely fused septum (Fig. 5E). Double-mutant gynoecia were strikingly abnormal despite the weak phenotypes of both *icu4-1/icu4-1* and *hst-1/hst-1* single-mutant plants. Major deformities were observed in most *icu4-1/icu4-1;hst-1/hst-1* gynoecia, which displayed reduced carpel fusion, incomplete septum formation, and production of stylar and stigmatic tissues at abnormal positions (Fig. 5F), as well as external placenta (which is an adaxial tissue in the wild type) bearing ovules, instead of the typical cells of the abaxial replum (Fig. 5, G and H). We observed a failure of the outer integument to completely cover the inner integument and the nucellus (Fig. 5H), indicating an alteration in the polarity of the outer integument. Lack of fusion in the septum was enhanced in double-mutant ovaries in which loss of transmitting tract can be observed (Fig. 5K), unlike those of the *hst-1/hst-1* single mutant (Fig. 5E). In addition, the replum of the double mutant was wider than those of the single mutants (Fig. 5K). In addition, other floral organs showed abnormal development. Stamens of wild type and *icu4-1/icu4-1* were indistinguishable and had pollen sacs in the adaxial surface (Fig. 5I), whereas a displacement to more lateral positions was occasionally observed in those of *icu4-1/icu4-1;hst-1/hst-1* double mutants (Fig. 5J). Taken together, the strong adaxial transformations developed in the double mutant suggest that the ICU4 product has an adaxializing function, which is in agreement with the adaxial transformations shown by plants containing the 35S::*ICU4*-G189D construct.

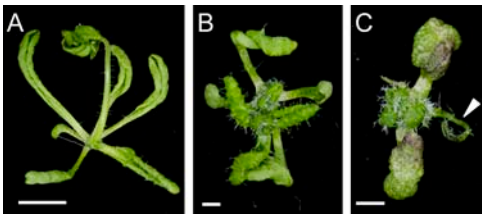

Figure 4. Rosettes of *icu4-1/icu4-1;hst-1/hst-1* plants. A to C, Rosettes of *hst-1/hst-1* (A) and *icu4-1/icu4-1;hst-1/hst-1* individuals (B and C), one of which developed a radialized leaf completely covered by trichomes (C; see arrowhead). Scale bars indicate 5 (A) and 1 (B and C) mm. Pictures were taken 21 d after sowing.

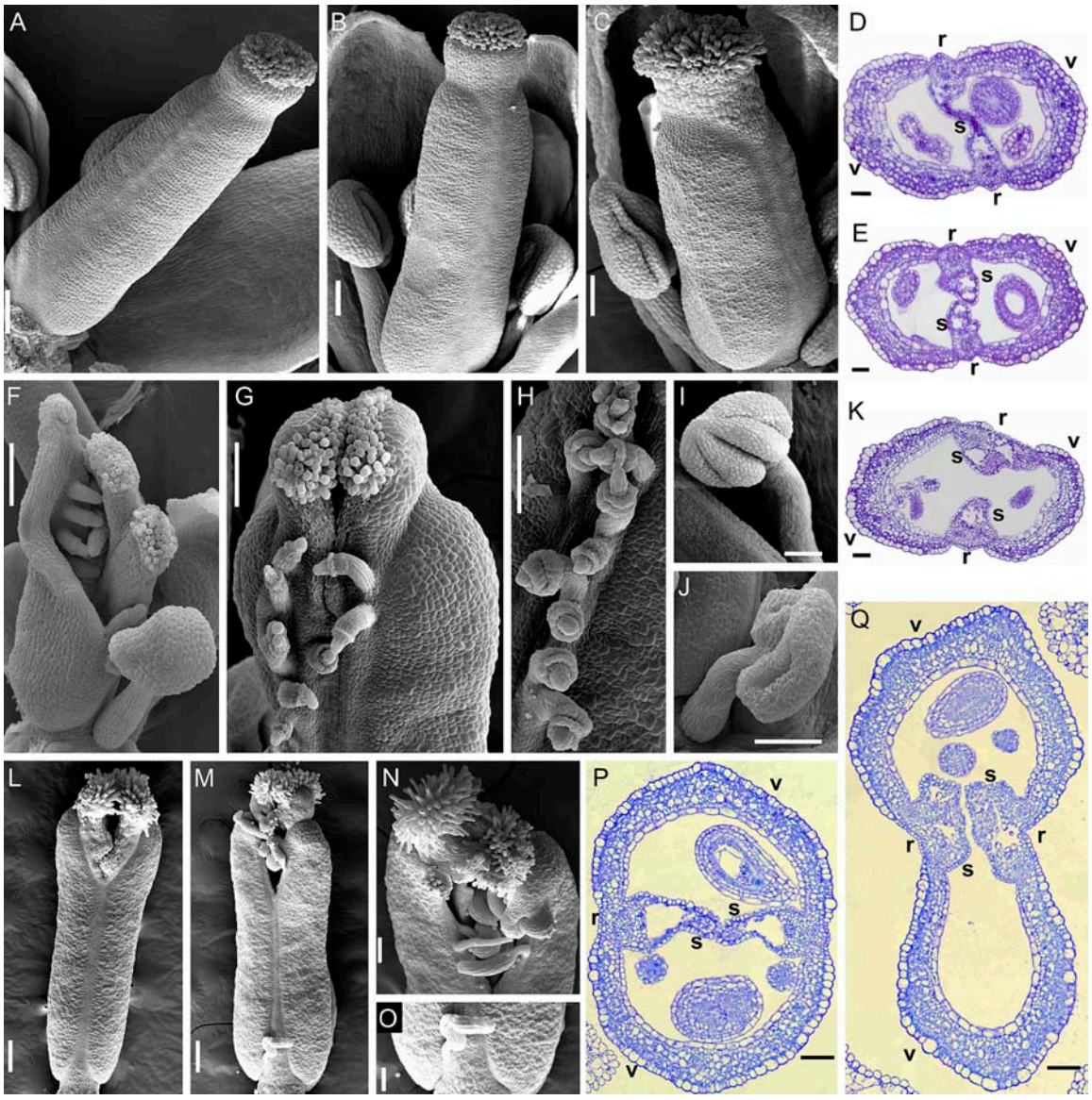

Figure 5. Scanning electron micrographs and histological sections of the gynoecia and ovaries of double mutants involving the *icu4-1* mutation. A to C, Scanning electron micrographs of En-2 (A), *icu4-1/icu4-1* (B), and *hst-1/hst-1* (C) gynoecia. D and E, Transverse sections of ovaries from *icu4-1/icu4-1* plants (D), which are indistinguishable from those of the wild type (data not shown) and present completely fused septa, whereas those of *hst-1/hst-1* are unfused (E). F to H, Gynoecia of *icu4-1/icu4-1*;*hst-1/hst-1* (F), which display ectopic placenta bearing ovules (G and H). I and J, The En-2 stamens (I) are indistinguishable from that of *icu4-1/icu4-1* (data not shown), whereas those of *icu4-1/icu4-1*;*hst-1/hst-1* double mutants (J) occasionally show the pollen sacs in lateral positions. K, Transverse sections of *icu4-1/icu4-1*;*hst-1/hst-1* ovaries. L to O, Siliques from a *crc-1/crc-1* single mutant (L) and *icu4-1/icu4-1*;*crc-1/crc-1* double mutants (M–O). The latter display more severe aberrations, as seen in the magnifications of the apical region (N) and the abaxial replum (O). P and Q, Transverse sections of ovaries from *crc-1/crc-1* (P) and *icu4-1/icu4-1*;*crc-1/crc-1* plants (Q). The septum of *crc-1/crc-1* fruits is not completely fused (P), whereas *icu4-1/icu4-1*;*crc-1/crc-1* double mutants have medially flattened siliques with a higher disconnection of the two pieces that form the septum (Q). r, Replum; s, septum; v, valve. Scale bars indicate 50 (D, E, K, P, and Q), 100 (A–C, F–J, N, and O), and 200 μm (L and M). Pictures were taken at stages 12 (prior to anthesis; A–C and F–J) and 14 (D, E, and K–Q).

Other Genetic Interactions

Other mutations have been described that determine the presence of ectopic ovules in the abaxial replum (Eshed et al., 1999, 2001). This is the case with double-mutant combinations involving alleles of *KAN1* (see introduction), *PICKLE/GYMNOS* (*PKL/GYM*; Ogas et al., 1997, 1999), which encodes a putative CHD3 chromatin remodeling factor, and the YABBY family member *CRABS CLAW* (*CRC*; Bowman and Smyth, 1999). To identify genetic interactions, we made double mutants with *icu4-1* and the *kan1-2*, *pkl-1*, or *crc-1* loss-of-function alleles. The *icu4-1/icu4-1*;

kan1-2/kan1-2 and *icu4-1/icu4-1;pkl-1/pkl-1* double mutants showed phenotypes that might be considered merely additive (data not shown).

Siliques from *icu4-1/icu4-1;crc-1/crc-1* double mutants showed a phenotype that was stronger than those of their *ICU4/ICU4;crc-1/crc-1* siblings. Plants homozygous for the strong *crc-1* allele displayed short and thick siliques that were opened at the apex (Fig. 5L) and had unfused septa (Fig. 5P). Ectopic ovules are displayed on the abaxial replum of *crc-1/crc-1* fruits at low frequency (Alvarez and Smyth, 1999). Double-mutant siliques showed a larger fissure in which ovules were easily seen (Fig. 5, M and N) and a higher frequency of ectopic ovules (Fig. 5, M and O). Eight of 30 fruits from three different double mutants displayed ectopic ovules, whereas none of the 30 *crc-1/crc-1* fruits derived from the same F_2 revealed this phenotype. In addition, *icu4-1/icu4-1;crc-1/crc-1* siliques were very wide and flat (Fig. 5Q) and their septa showed a stronger disconnection than those of *crc-1/crc-1* siliques (Fig. 5P). Thus, the mutant phenotype caused by homozygosis of *crc-1* is enhanced by the gain-of-function allele *icu4-1*.

Expression Analysis

We detected *ICU4* transcripts in roots, vegetative leaves, shoots, flower buds, and open flowers of Col-0 by semiquantitative reverse transcription (RT)-PCR (Fig. 6A). Quantitative, real-time RT-PCR (qRT-PCR) amplifications were also performed using RNA from flowers, leaves, and aerial tissues (whole plants with no roots) of En-2 and *icu4-1/icu4-1* plants (Fig. 6B). Transcript levels of *ICU4* were lower in the leaves than in the aerial tissues of En-2. However, transcript levels were 8-fold higher in *icu4-1/icu4-1* leaves than in En-2 leaves, as is to be expected if *icu4-1* escapes cleavage by the miRNA machinery, but only 2-fold in the aerial tissues of the mutant compared with those of the wild type. Further qRT-PCR expression analyses were made separately for leaves of the first and second, third to fifth, and sixth to last vegetative nodes, as well as for roots, shoots, and shoot apices of En-2 and *icu4-1* homozygotes (Fig. 6, C and D). Overexpression of the gene was higher in the first two leaves of the *icu4-1* mutant (Fig. 6D), consistent with the more severe phenotype displayed by these leaves (Fig. 2, B and F). *ICU4* was also overexpressed in mutant shoots, roots, and shoot apical meristems (Fig. 6C).

Meristematic activity due to ectopic expression of class I *KNOX* genes (Chuck et al., 1996; Gallois et al., 2002) might explain the outgrowths seen in *icu4-1/icu4-1* leaves. Consequently, we studied by qRT-PCR the expression of *KNAT1*, *KNAT2*, and *KNAT6* (Lincoln et al., 1994; Semiarti et al., 2001). In addition, an indirect effect of the *icu4-1* allele on the expression of class I *KNOX* genes is possible by the negative regulation of abaxializing genes. The *YABBY* genes, for instance, repress the expression of *KNOX* genes (Kumaran et al., 2002). Therefore, we also quantitated

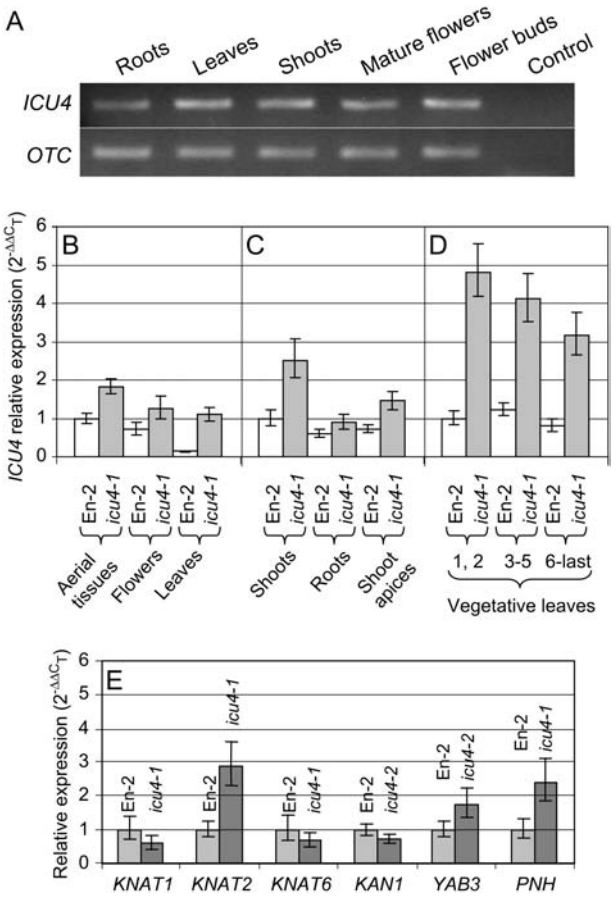

Figure 6. Expression analysis of *ICU4* and other genes in En-2 and *icu4/icu4* plants. A, Semiquantitative RT-PCR visualization of *ICU4* expression in assorted organs. B to D, qRT-PCR expression analyses of *ICU4* in En-2 and *icu4-1/icu4-1* plants. Bars indicate expression levels for the *ICU4* gene, which were previously normalized with those of the housekeeping gene *ORNITHINE TRANSCARBAMILASE*, referred to as those obtained in aerial tissues (whole plants without roots; B), shoots (C), and first- and second-node leaves (D) of En-2, to which a value of 1 was given. Tissues were collected 21 (vegetative leaves, shoot apical meristems, and roots), 30 (aerial tissues and flowers), and 38 (shoots) d after sowing. E, qRT-PCR expression analyses of the *KAN1*, *YAB3*, class I *KNOX* genes, and *PNH* in *icu4-1/icu4-1* or *icu4-2/icu4-2* leaves, referred to as En-2 leaves, to which a value of 1 was given. Leaves were collected 21 d after sowing.

the expression of the abaxializing *KAN1* (Eshed et al., 2001) and *YAB3* (Kumaran et al., 2002) genes. Only *KNAT2* was found to be misexpressed, with a 3-fold up-regulation in mutant leaves (Fig. 6E).

Overexpression of *PINHEAD* (*PNH*) has been described as causing leaf incurvature, most likely due to increased cell division in the abaxial domain (Newman et al., 2002). *PNH* encodes a member of the Argonaute protein family that is expressed in the shoot apical meristem, provascular tissues, and the adaxial domain of wild-type leaf primordia (Lynn et al., 1999; Newman et al., 2002). We studied the expression of *PNH* by qRT-PCR and found a 2.4-fold up-regulation in *icu4-1/icu4-1* leaves (Fig. 6E).

DISCUSSION

icu4-1 and *icu4-2* Are Gain-of-Function Alleles of the *ICU4* Gene

We used the identical *icu4-1* and *icu4-2* semidominant mutations (Serrano-Cartagena et al., 2000) to positionally clone the *ICU4* gene, which encodes the ATHB15 transcription factor, an HD-Zip III family member. A dosage analysis performed in triploids indicated that *icu4-1* is a gain-of-function allele and constitutive overexpression of *icu4-1* in transgenic plants with a wild-type background caused an extreme phenotype. The latter might be due to the generalized transcription driven by the 35S promoter, whereas expression of the endogenous *ICU4* gene is restricted to specific organs and tissues. In addition, the mutant phenotype of *icu4-1/icu4-1* individuals was suppressed by an RNAi construct designed to target transcripts of the *ICU4* gene. Taken together, these results show that *icu4-1* and *icu4-2* are gain-of-function alleles of the *ICU4* gene. Given that expression of this gene is known to be spatially restricted in wild-type plants (Prigge et al., 2005; Williams et al., 2005), the gain of function of semidominant *icu4* alleles can be explained by ectopic derepression or by an increase in transcript levels within the wild-type realm of action of the gene.

A Point Mutation at a miRNA Complementarity Site Causes Overexpression of the *ICU4* Gene

All the gain-of-function mutations described so far in the HD-Zip III family members *PHB*, *PHV*, and *REV* lie within the region that encodes the START domain of their protein products. However, the presence within this region of a sequence complementary to two miRNAs that differ in a single nucleotide, miR165 and miR166 (Rhoades et al., 2002), made disruption of miRNA-mRNA pairing the most likely explanation for the phenotype of semidominant *phb*, *phv*, and *rev* alleles (for review, see Bowman, 2004). The transcripts of HD-Zip III genes are cleaved at the miRNA complementarity site in a variety of plant species, indicating that this posttranscriptional regulatory mechanism dates back more than 400 million years (Floyd and Bowman, 2004).

The *icu4-1* and *icu4-2* alleles bear the same nucleotide substitution, a G-to-A transition affecting the miR165/166 complementarity site of *ICU4*, identical to those already described for several semidominant alleles of *PHB* and *PHV*. The miR165/166 complementarity site is mutated also in gain-of-function alleles of other HD-Zip III family members, such as *REV* and *rld1* (Emery et al., 2003; Juarez et al., 2004; Zhong and Ye, 2004). Consequently, defective cleavage of mutant transcripts due to impaired miRNA-mRNA pairing provides a molecular explanation for the gain of function of *icu4-1* and *icu4-2*. Cleavage of *ATHB15* transcripts mediated by miR166 has been recently demonstrated in vivo (Kim et al., 2005).

Impaired miRNA-mRNA pairing causes accumulation of *ICU4* transcripts, as indicated by its up-regulation in all the tissues studied in the *icu4-1* mutant, which was higher in organs with a more conspicuous phenotype, such as leaves and shoots. The severity of leaf morphological aberrations correlated with the level of *ICU4* overexpression, which was higher in juvenile leaves. Weaker incurvature and less overexpression were seen in leaves from the third to the adult nodes. A different result was obtained by Green et al. (2005) with the *cna-1* mutant, in which *CNA* mRNA levels were similar to those of the wild type. The putative dominant negative *cna-1* allele carries a point mutation in a conserved domain of *CNA* different from that containing the miRNA complementarity site (Green et al., 2005).

The *ICU4* Gene Is Required for Shoot and Root Apical Meristem Patterning and Stem Vascular Differentiation

Based on the phenotypic characterization of the *icu4-1 hst-5* double mutants, we previously proposed that *ICU4* might play a role in regulating shoot apical meristem function (Serrano-Cartagena et al., 2000). The shoot apical meristem was also impaired in our *icu4-1* and *icu4-2* single mutants, as inferred from their abnormal phyllotaxis, paired cauline leaves, and axillary shoots, and occasionally seen twin rosettes. This result, along with the enlarged shoot meristems seen in *clv cna* double mutants and the triple null *phb phv cna* (Green et al., 2005; Prigge et al., 2005), indicates a role for the *ICU4* gene in shoot meristem function.

Several HD-Zip III genes are known to be required for lateral root development (Hawker and Bowman, 2004) and shoot radial patterning (Emery et al., 2003; Zhong and Ye, 2004). Consistent with this, *ICU4* also has a role in patterning shoot vascular bundles, as indicated by the overproliferation of metaxylem tracheids, the development of extra procambium layers, and the frequent reduction in the number of vascular bundles observed in the shoots of *icu4-1/icu4-1* plants. Our results go along with those of Ohashi-Ito and Fukuda (2003), who characterized the expression profile of the *ATHB15* gene of Arabidopsis and that of its Zinnia ortholog *ZeHB-13*, which were found to be involved in the differentiation of procambial and xylem cells, where they are expressed. Thus, both genes might act as transcriptional regulators in early vasculature development.

Although the *ATHB15* promoter drives the expression of a reporter gene in the vascular cell files that start next to the quiescent center of primary root meristems (Ohashi-Ito and Fukuda, 2003), no root phenotypes have been described to be a consequence of perturbations in *ATHB15* function. We have found that roots of *icu4-1* homozygotes are shorter, initiate more secondary roots, and contain longer root hairs than the wild type and display an aberrant cell pattern in the root apical meristem.

The ATHB15 Transcription Factor Has Adaxializing Activity

Dorsoventral polarity, a property of plant lateral organs such as leaves and floral organs, is thought to depend on an adaxializing signal emanating from the shoot apical meristem (Sussex, 1954). The adaxial and abaxial domains of developing lateral organs are patterned by the activities of HD-Zip III adaxializing factors, and KANADI and YABBY abaxializing factors (Eshed et al., 1999; Siegfried et al., 1999; Kerstetter et al., 2001; Kumaran et al., 2002; Emery et al., 2003). As proposed in the model of Waites and Hudson (1995), the flatness of the leaf lamina would be explained by localized growth at locations where the adaxial and abaxial identities meet.

The expression of *REV*, *PHV*, *PHB*, and *ATHB15* is restricted to the adaxial domains of lateral organ primordia (McConnell et al., 2001; Otsuga et al., 2001; Prigge et al., 2005; Williams et al., 2005). On the contrary, members of the KANADI and YABBY families are expressed abaxially in lateral organs (Sawa et al., 1999a, 1999b; Siegfried et al., 1999; Eshed et al., 2001; Kerstetter et al., 2001). Consistent with the model of Waites and Hudson (1995), gain-of-function *phv*, *phb*, and *rev* mutants have adaxialized leaves (McConnell and Barton, 1998; McConnell et al., 2001; Emery et al., 2003; Zhong and Ye, 2004). Furthermore, loss-of-function *kan* alleles cause abaxial tissue reduction together with an expansion of the realm of expression of *REV*, *PHB*, and *PHV* (Eshed et al., 1999, 2001).

The *icu4-1* and *icu4-2* gain-of-function mutations delay juvenile-to-adult phase change and flowering and increase the number of vegetative leaves, which lack abaxial trichomes. These phenotypic traits are the opposite of those associated with loss-of-function *hst* mutations, which accelerate phase change and cause early flowering and the presence of abaxial trichomes on juvenile leaves (Telfer and Poethig, 1998; Serrano-Cartagena et al., 2000; Bollman et al., 2003). These observations suggest that the *ICU4* and *HST* genes are involved in related processes, an idea reinforced by the synergistic phenotype of the *icu4-1 hst-5* (Serrano-Cartagena et al., 2000) and *icu4-1 hst-1* (this work) double mutants. Given that loss-of-function *hst* mutations reduce miRNA levels (Park et al., 2005), their mutant phenotype is expected to be pleiotropic as a consequence of the simultaneous overexpression of different miRNA target genes, which might include *ICU4*.

Leaves of the *icu4-1 hst-1* double mutant were helically rotated and occasionally radialized and presented many trichomes, suggesting that they are partially adaxialized. Also, the recessed outer integuments of the mature ovules of these double mutants were reminiscent of those caused by mutations in the *INNER NO OUTER* (*INO*) gene, a member of the YABBY family that is essential for the formation and asymmetric growth of the ovule outer integument (Villanueva et al., 1999). These observations, together with the synergistic phenotype of the *ago1-51 icu4-1* double mutant, which displays adaxialized leaves (S. Jover-Gil, H. Candela, J.M. Barrero, P. Robles, J.L. Micol, and M.R. Ponce, unpublished data), and the adaxial transformations observed in 35S::*ICU4*-G189D transformants support the notion that *ICU4* has an adaxializing activity. Although it has been previously suggested that the *CNA* (*ICU4*) gene might be involved in specifying polarity, this role did not become obvious from the study of *cna* loss-of-function alleles (Prigge et al., 2005).

Fruits of the *hst-1* mutant, which are medially flattened and occasionally opened at the apical end, show some resemblance to those of homozygotes for loss-of-function alleles of the *CRC* gene (Alvarez and Smyth, 1999), a YABBY family member that is required for abaxial cell fate specification in developing carpels (Bowman and Smyth, 1999). Whereas *crc* single mutants do not show a clear loss-of-abaxial fate phenotype, their double-mutant combinations with *kan1* alleles condition the presence of an external placenta with ovules, indicating that both genes cooperate to promote abaxial identity in carpels (Eshed et al., 1999). External ovules in the medial domain of the carpels are also observed in *kan1 hst* double mutants (Eshed et al., 2001), which show a synergistic interaction, suggesting that *HST* works in parallel with *KAN1* in the specification of lateral organ polarity (Bollman et al., 2003). Interestingly, gynoecia of *icu4-1 hst-1* double mutants show a similar strong interaction and often display the replacement of the abaxial replum by a placenta with ovules. In addition, siliques of *icu4-1 crc-1* double mutants show an enhancement of the mutant phenotype conferred by the *crc-1* allele. These phenotypes further indicate that *ICU4* has an adaxializing activity.

As expected from the predicted impairment of miRNA-mediated regulation caused by the *icu4-1* mutation, *ICU4* itself was found to be up-regulated in the *icu4-1* mutant. We found that leaf incurvature is at least partially caused by ectopic *PNH* expression in the *icu4-1* mutant, which in turn indicates a positive regulatory effect of *ICU4* on *PNH*. The *KNAT2* meristematic gene was also found up-regulated in *icu4-1/icu4-1* leaves, suggesting that *ICU4* also promotes meristematic activity, which might account for the abaxial protuberances observed in the mutant leaves.

MATERIALS AND METHODS

Plant Materials, Growth Conditions, and Crosses

Several Arabidopsis (*Arabidopsis thaliana* L. Heyhn.) lines studied in this work were supplied by the Nottingham Arabidopsis Stock Centre. These include the En-2 wild type, the N400 and N401 mutants (respectively carrying the *icu4-1* and *icu4-2* alleles, both in an En-2 genetic background), the N517186 and N513134 T-DNA insertion lines (respectively carrying the *icu4-3* and *icu4-4* alleles), and the N523733, N565586, and N579212 T-DNA insertion lines (which we named *athb8-3*, *athb8-4*, and *athb8-5*, given that the only *ATHB8* alleles already published are *athb8-1* and *athb8-2*), which are described at the SIGnAL Web site (Alonso et al., 2003; http://signal.salk.edu), and the *crc-1*, *pkl-1*, and *hst-1* mutants. The CS3151 tetraploid line was supplied by the Arabidopsis Biological Resource Centre. The *kan1-2* mutant was provided by J.L. Bowman, and the p*ATHB-8-GUS* transgenic line by S. Baima.

Cultures were performed as described by Ponce et al. (1998), at 20°C ± 1°C and 60% to 70% relative humidity under continuous illumination of 7,000 lux. Crosses were performed as described in Berná et al. (1999). For dosage analysis, tetraploid CS3151 plants were fertilized with *icu4-1* pollen.

Positional Cloning, Sequencing, and Sequence Analysis

Mapping was carried out as described by Ponce et al. (1999). Based on the genome sequence available at the Cereon database (http://www.arabidopsis.org/Cereon), we developed 12 new single-nucleotide polymorphism and insertion/deletion markers within the candidate region (Supplemental Table II), which were used to screen for informative recombinants. PCR products spanning the At1g52150 gene from En-2, *icu4-1*, and *icu4-2* homozygotes were sequenced in 5-μL reactions using internal primers and the ABI PRISM BigDye terminator cycle sequencing kit. Sequencing electrophoreses were performed on an ABI PRISM 3100 genetic analyzer.

Amino acid sequences of HD-Zip III family members were aligned using ClustalX, version 1.5b, and shaded with Boxshade 3.21 (http://www.ch.embnet.org/software/BOX_form.html). Identity and similarity percentages were obtained by aligning protein sequences; those for the miR165/166 complementarity site were obtained by aligning nucleotide sequences, whose accession numbers were as follows: ICU4 (ATHB-15; NP_175627.1), ATHB-8 (NP_195014.1), ATHB-14 (PHB; NP_181018.1), REV (IFL1; NP_200877.1), ATHB-9 (PHV; NP_174337.1), ZeHB-13 (BAD01502.1), ZeHB-2 (CAC84276.1), *ICU4* (NM_104096.2), *ZeHB-2* (AJ312054.1), *ZeHB-13* (AB109562.1), *ATHB-8* (NM_119441.3), *ATHB-9* (*PHV*; NM_102785.3), *ATHB-14* (*PHB*; NM_129025.2), *REV* (NM_125462.2), *rld1* (AY501430.1), *ZeHB-1* (AJ312053.1), *ZeHB-3* (AJ312055.1), *ZeHB-10* (AB084380.1), *ZeHB-11* (AB084381.1), *ZeHB-12* (AB084382.1), *Hox9* (AY423716.1), *Hox10* (AY425991.1), *PpHB10* (AB032182.1), and *HB-1* (AY497772.1).

Microscopy

Whole-rosette and single-leaf pictures were taken in a MZ6 stereomicroscope (Leica) or in a SMZ800 stereomicroscope (Nikon). For light microscopy, plant material was fixed with formaldehyde acetic acid/Triton (1.85% formaldehyde, 45% ethanol, 5% glacial acetic acid, and 1% Triton X-100) and embedded in JB4 resin (Electron Microscopy Sciences) as described in Serrano-Cartagena et al. (2000). Transverse sections of 5-μm leaves or 3- to 4-μm siliques were made on a microtome (Microm International HM350S), stained with 0.1% toluidine blue, and observed under brightfield illumination using a DMRB microscope (Leica) equipped with a DXM1200 digital camera (Nikon) or an Eclipse E800 microscope (Nikon) equipped with a COLORVIEW-III digital camera (Nikon).

Root confocal microscopy was performed as detailed in Pérez-Pérez et al. (2002). Brightfield micrographs of leaf venation patterns were obtained as described in Candela et al. (1999). Scanning electron microscopy was performed as described in Serrano-Cartagena et al. (2000) for vegetative tissues and in Ripoll et al. (2006) for reproductive tissues.

Generation of Transgenic Plants

The 35S::*ICU4* construct was made by placing the *ICU4* cDNA under the control of the tandemly repeated 35S promoter of the pBIN-JIT vector (Ferrándiz et al., 2000). The full-length wild-type *ICU4* cDNA was obtained from the RIKEN Genomic Sciences Center (clone RAFL09-35-K18; Seki et al., 1998, 2002). The 35S::*ICU4*-G189D construct, which consisted in the *icu4-1* mutant allele cloned into pBIN-JIT, was generated after PCR amplification of the RAFL09-35-K18 clone with two primer pairs. Two of these primers were designed to create a G-to-A transition in the fifth position of the fifth exon of *ICU4* (5′-CTGGAATGAAGCCTGATCCGGATTCCATTGG-3′ and its exact complement). The 35S::*ICU4*-RNAi construct was designed for RNAi and included a genomic fragment of the coding region of the wild-type *ICU4* allele amplified using the primers 5′-CTTCGGTTCTGAAACCACAC-3′ and 5′-TGTGATTTGTGAAGCTACTCC-3′. The PCR amplification product was ligated in sense and antisense orientations into pCF6 (C. Ferrándiz, unpublished data), both fragments being separated by the sixth intron of the *FRUITFULL* gene (Gu et al., 1998) and then transferred to pBIN-JIT for Agrobacterium-mediated transformation.

All constructs obtained in this work were fully sequenced to confirm their structural integrity prior to being transferred into plants by the floral-dip method (Clough and Bent, 1998). Transgenic plants were selected on 50 μg/mL kanamycin-supplemented medium (Weigel and Glazebrook, 2002).

RNA Isolation and RT-PCR Analyses

Total RNA was extracted from plant material, which was collected, immediately frozen in liquid N_2, and stored at −80°C. RNA was extracted with TRIzol (Invitrogen) and further purified with an RNeasy plant mini kit (Qiagen), according to the instructions of the manufacturers. RNA concentration was determined in a spectrophotometer and its quality checked by visualization in an agarose gel.

For semiquantitative RT-PCR, RNA was extracted from 80 to 100 mg of roots, vegetative leaves, shoots, mature flowers, and flower buds of Col-0, collected 21 (roots and vegetative leaves) and 30 (shoots, mature flowers, and flower buds) d after sowing. First-strand cDNA was synthesized with random hexamers using the SuperScript first-strand synthesis kit, according to the manufacturer's instructions (Invitrogen). PCR amplifications were performed as described in Pérez-Pérez et al. (2004). The housekeeping *ORNITHINE TRANSCARBAMILASE* gene (Quesada et al., 1999) was used as a positive control.

For qRT-PCR, RNA was isolated from 50 to 100 mg of plant material collected 21 (vegetative leaves, shoot apices, and roots), 30 (flowers and aerial tissues), and 38 (shoots) d after sowing. qRT-PCR was performed using first-strand cDNA as a template on an ABI PRISM 7000 sequence detection system (Perkin-Elmer/Applied Biosystems). The primers used are shown in Supplemental Table II. Amplification reactions and relative quantification of gene expression data were carried out as described in Livak and Schmittgen (2001), Cnops et al. (2004), and Pérez-Pérez et al. (2004).

ACKNOWLEDGMENTS

We wish to thank P. Robles and V. Quesada for comments on the manuscript, J.M. Serrano, V. García-Sempere, M.A. Climent, and M.D. Segura for technical assistance, the Salk Institute Genomic Analysis Laboratory for providing the sequence-indexed Arabidopsis T-DNA insertion mutants, the RIKEN Genomic Sciences Center for providing the *ICU4* cDNA, and J.L. Bowman and S. Baima for kindly providing mutant or transgenic lines.

Received January 17, 2006; revised March 16, 2006; accepted April 7, 2006; published April 14, 2006.

LITERATURE CITED

Alonso JM, Stepanova AN, Leisse TJ, Kim CJ, Chen H, Shinn P, Stevenson DK, Zimmerman J, Barajas P, Cheuk R, et al (2003) Genome-wide insertional mutagenesis of *Arabidopsis thaliana*. Science **301:** 653–657

Alvarez J (1994) The *SPITZEN* gene. *In* J Bowman, ed, Arabidopsis: An Atlas of Morphology and Development. Springer-Verlag, New York, pp 188–189

Alvarez J, Smyth DR (1999) *CRABS CLAW* and *SPATULA*, two Arabidopsis genes that control carpel development in parallel with *AGAMOUS*. Development **126:** 2377–2386

Baima S, Nobili F, Sessa G, Lucchetti S, Ruberti I, Morelli G (1995) The expression of the *Athb-8* homeobox gene is restricted to provascular cells in *Arabidopsis thaliana*. Development **121:** 4171–4182

Bartel B, Bartel DP (2003) miRNAs: at the root of plant development? Plant Physiol **132:** 709–717

Bartel DP (2004) miRNAs: genomics, biogenesis, mechanism, and function. Cell **116:** 281–297

Bartel DP, Chen CZ (2004) Micromanagers of gene expression: the potentially widespread influence of metazoan microRNAs. Nat Rev Genet **5:** 396–400

Baulcombe D (2004) RNA silencing in plants. Nature **16:** 356–363

Berná G, Robles P, Micol JL (1999) A mutational analysis of leaf morphogenesis in Arabidopsis. Genetics **152:** 729–742

Bohnsack MT, Czaplinski K, Gorlich D (2004) Exportin 5 is a RanGTP-dependent dsRNA-binding protein that mediates nuclear export of pre-miRNAs. RNA **10:** 185–191

Bollman KM, Aukerman MJ, Park MY, Hunter C, Berardini TZ, Poethig RS (2003) *HASTY*, the Arabidopsis ortholog of exportin 5/MSN5, regulates phase change and morphogenesis. Development **130:** 1493–1504

Bowman JL (2004) Class III HD-Zip gene regulation, the golden fleece of ARGONAUTE activity? Bioessays **26:** 938–942

Bowman JL, Smyth DR (1999) *CRABS CLAW*, a gene that regulates carpel and nectary development in Arabidopsis, encodes a novel protein with zinc finger and helix-loop-helix domains. Development **126:** 2387–2396

Bürger D (1971) Die morphologischen mutanten des Göttinger Arabidopsis-sortiments, einschlieslich der mutanten mit abweichender samenfarbe. Arabidopsis Inf Serv **8:** 36–42

Candela H, Martínez-Laborda A, Micol JL (1999) Venation pattern formation in Arabidopsis vegetative leaves. Dev Biol **205:** 205–216

Chen X (2005) MicroRNA biogenesis and function in plants. FEBS Lett **579:** 5923–5931

Chuck G, Lincoln C, Hake S (1996) *KNAT1* induces lobed leaves with ectopic meristems when overexpressed in Arabidopsis. Plant Cell **8:** 1277–1289

Clough SJ, Bent AF (1998) Floral dip: a simplified method for Agrobacterium-mediated transformation of Arabidopsis. Plant J **16:** 735–743

Cnops G, Jover-Gil S, Peters J, Neyt P, De Block S, Robles P, Ponce MR, Gerats T, Micol JL, Van Lijsebettens M (2004) The *rotunda2* mutants identify a role for the *LEUNIG* gene in vegetative leaf morphogenesis. J Exp Bot **55:** 1529–1539

Du T, Zamore PD (2005) microPrimer: the biogenesis and function of microRNA. Development **132:** 4645–4652

Dugas DV, Bartel B (2004) microRNA regulation of gene expression in plants. Curr Opin Plant Biol **7:** 512–520

Emery JF, Floyd SK, Alvarez J, Eshed Y, Hawker NP, Izhaki A, Baum SF, Bowman JL (2003) Radial patterning of Arabidopsis shoots by class III HD-ZIP and KANADI genes. Curr Biol **13:** 1768–1774

Eshed Y, Baum SF, Bowman JL (1999) Distinct mechanisms promote polarity establishment in carpels of Arabidopsis. Cell **99:** 199–209

Eshed Y, Baum SF, Perea JV, Bowman JL (2001) Establishment of polarity in lateral organs of plants. Curr Biol **11:** 1251–1260

Ferrándiz C, Liljegren SJ, Yanofsky MF (2000) Negative regulation of the *SHATTERPROOF* genes by FRUITFULL during Arabidopsis fruit development. Science **289:** 436–438

Ferrándiz C, Pelaz S, Yanofsky MF (1999) Control of carpel and fruit development in Arabidopsis. Annu Rev Biochem **68:** 321–354

Floyd SK, Bowman JL (2004) Gene regulation: ancient miRNA target sequences in plants. Nature **428:** 485–486

Gallois J-L, Woodward C, Reddy GV, Sablowsky R (2002) Combined *SHOOTMERISTEMLESS* and *WUSCHEL* trigger ectopic organogenesis in Arabidopsis. Development **129:** 3207–3217

Green KA, Prigge MJ, Katzman RB, Clark SE (2005) *CORONA*, a member of the class III homeodomain leucine zipper gene family in Arabidopsis regulates stem cell specification and organogenesis. Plant Cell **17:** 691–704

Gu Q, Ferrándiz C, Yanofsky MF, Martienssen R (1998) The *FRUITFULL* MADS-box gene mediates cell differentiation during Arabidopsis fruit development. Development **125:** 1509–1517

Gwizdek C, Ossareh-Nazari B, Brownawell AM, Doglio A, Bertrand E, Macara IG, Dargemont C (2003) Exportin-5 mediates nuclear export of minihelix-containing RNAs. J Biol Chem **278:** 5505–5508

Hawker NP, Bowman JL (2004) Roles for class III HD-Zip and KANADI genes in Arabidopsis root development. Plant Physiol **135:** 2261–2270

Heisler MG, Ohno C, Das P, Sieber P, Reddy GV, Long JA, Meyerowitz EM (2005) Patterns of auxin transport and gene expression during primordium development revealed by live imaging of the Arabidopsis inflorescence meristem. Curr Biol **15:** 1899–1911

Hunter C, Poethig RS (2003) miSSING LINKS: miRNAs and plant development. Curr Opin Genet Dev **13:** 372–378

Jover-Gil S, Candela H, Ponce MR (2005) Plant microRNAs and development. Int J Dev Biol **49:** 733–744

Juarez MT, Kui JS, Thomas J, Heller BA, Timmermans MC (2004) miRNA-mediated repression of *rolled leaf1* specifies maize leaf polarity. Nature **428:** 84–88

Kang J, Dengler N (2002) Cell cycling frequency and expression of the homeobox gene ATHB-8 during leaf vein development in Arabidopsis. Planta **216:** 212–219

Kang J, Tang J, Donnelly P, Dengler N (2003) Primary vascular pattern and expression of *ATHB-8* in shoots of Arabidopsis. New Phytol **158:** 443–454

Kerstetter RA, Bollman K, Taylor RA, Bomblies K, Poethig RS (2001) *KANADI* regulates organ polarity in Arabidopsis. Nature **411:** 706–709

Kim J, Jung J-H, Reyes JL, Kim Y-S, Kim S-Y, Chung K-S, Kim JA, Lee M, Lee Y, Kim VN, et al (2005) microRNA-directed cleavage of *ATHB15* mRNA regulates vascular development in Arabidopsis inflorescence stems. Plant J **42:** 84–94

Kim VN (2005) MicroRNA biogenesis: coordinated cropping and dicing. Nat Rev Mol Cell Biol **6:** 376–385

Kranz AR (1978) Demonstration of new and additional population samples and mutant lines of the AIS-seed bank. Arabidopsis Inf Serv **15:** 118–139

Kumaran MK, Bowman JL, Sundaresan V (2002) YABBY polarity genes mediate the repression of *KNOX* homeobox genes in Arabidopsis. Plant Cell **14:** 2761–2770

Lincoln C, Long J, Yamaguchi J, Serikawa K, Hake S (1994) A *knotted1*-like *homeobox* gene in Arabidopsis is expressed in the vegetative meristem and dramatically alters leaf morphology when overexpressed in transgenic plants. Plant Cell **6:** 1859–1876

Livak KJ, Schmittgen TD (2001) Analysis of relative gene expression data using real-time quantitative PCR and the $2^{-\Delta\Delta C_T}$ method. Methods **25:** 402–408

Lynn K, Fernandez A, Aida M, Sedbrook J, Tasaka M, Masson P, Barton MK (1999) The *PINHEAD/ZWILLE* gene acts pleiotropically in Arabidopsis development and has overlapping functions with the *ARGONAUTE1* gene. Development **126:** 469–481

McConnell JR, Barton MK (1998) Leaf polarity and meristem formation in Arabidopsis. Development **125:** 2935–2942

McConnell JR, Emery J, Eshed Y, Bao N, Bowman J, Barton MK (2001) Role of *PHABULOSA* and *PHAVOLUTA* in determining radial patterning in shoots. Nature **411:** 709–713

Newman KL, Fernandez AG, Barton MK (2002) Regulation of axis determinacy by the Arabidopsis *PINHEAD* gene. Plant Cell **14:** 3029–3042

Ogas J, Cheng JC, Sung ZR, Somerville C (1997) Cellular differentiation regulated by gibberellin in the *Arabidopsis thaliana pickle* mutant. Science **277:** 91–94

Ogas J, Kaufmann S, Henderson J, Somerville C (1999) PICKLE is a CHD3 chromatin-remodeling factor that regulates the transition from embryonic to vegetative development in Arabidopsis. Proc Natl Acad Sci USA **96:** 13839–13844

Ohashi-Ito K, Fukuda H (2003) HD-zip III homeobox genes that include a novel member, *ZeHB-13* (Zinnia)/*ATHB-15* (Arabidopsis), are involved in procambium and xylem cell differentiation. Plant Cell Physiol **44:** 1350–1358

Otsuga D, DeGuzman B, Prigge MJ, Drews GN, Clark SE (2001) *REVOLUTA* regulates meristem initiation at lateral positions. Plant J **25:** 223–236

Papp I, Mette MF, Aufsatz W, Daxinger L, Schauer E, Ray A, van der Winden J, Matzke M, Matzke AJ (2003) Evidence for nuclear processing of plant micro RNA and short interfering RNA precursors. Plant Physiol **132:** 1382–1390

Park MY, Wu G, Gonzalez-Sulser A, Vaucheret H, Poethig RS (2005) Nuclear processing and export of microRNAs in Arabidopsis. Proc Natl Acad Sci USA **102:** 3691–3696

Pérez-Pérez JM, Ponce MR, Micol JL (2002) The *UCU1* Arabidopsis gene encodes a SHAGGY/GSK3-like kinase required for cell expansion along the proximodistal axis. Dev Biol **242:** 161–173

Pérez-Pérez JM, Ponce MR, Micol JL (2004) The *ULTRACURVATA2* gene of Arabidopsis encodes an FK506-binding protein involved in auxin and brassinosteroid signaling. Plant Physiol **134:** 101–117

Ponce MR, Quesada V, Micol JL (1998) Rapid discrimination of sequences flanking and within T-DNA insertions in the Arabidopsis genome. Plant J **14:** 497–501

Ponce MR, Robles P, Micol JL (1999) High-throughput genetic mapping in Arabidopsis. Mol Gen Genet **261:** 408–415

Ponting CP, Aravind L (1999) START: a lipid-binding domain in StAR, HD-ZIP and signalling proteins. Trends Biochem Sci **24:** 130–132

Prigge MJ, Otsuga D, Alonso JM, Ecker R, Drews GN, Clark SE (2005) Class III homeodomain-leucine zipper gene family members have overlapping, antagonistic, and distinct roles in Arabidopsis development. Plant Cell **17:** 61–76

Quesada V, Ponce MR, Micol JL (1999) *OTC* and *AUL1*, two convergent and overlapping genes in the nuclear genome of *Arabidopsis thaliana*. FEBS Lett **461:** 101–106

Rhoades MW, Reinhart BJ, Lim LP, Burge CB, Bartel B, Bartel DP (2002) Prediction of plant miRNA targets. Cell **110:** 513–520

Ripoll JJ, Ferrándiz C, Martínez-Laborda A, Vera A (2006) *PEPPER*, a novel K-homology domain gene, regulates vegetative and gynoecium development in Arabidopsis. Dev Biol **289:** 346–359

Sawa S, Ito T, Shimura Y, Okada K (1999a) *FILAMENTOUS FLOWER* controls the formation and development of Arabidopsis inflorescences and floral meristems. Plant Cell **11:** 69–86

Sawa S, Watanabe K, Goto K, Liu YG, Shibata D, Kanaya E, Morita EH, Okada K (1999b) *FILAMENTOUS FLOWER*, a meristem and organ identity gene of Arabidopsis, encodes a protein with a zinc finger and HMG-related domains. Genes Dev **13:** 1079–1088

Schrick K, Nguyen D, Karlowski WM, Mayer KF (2004) START lipid/sterol-binding domains are amplified in plants and are predominantly associated with homeodomain transcription factors. Genome Biol **5:** R41

Seki M, Carninci P, Nishiyama Y, Hayashizaki Y, Shinozaki K (1998) High-efficiency cloning of Arabidopsis full-length cDNA by biotinylated CAP trapper. Plant J **15:** 707–720

Seki M, Narusaka M, Kamiya A, Ishida J, Satou M, Sakurai T, Nakajima M, Enju A, Akiyama K, Oono Y, et al (2002) Functional annotation of a full-length Arabidopsis cDNA collection. Science **296:** 141–145

Semiarti E, Ueno Y, Tsukaya H, Iwakawa H, Machida C, Machida Y (2001) The *ASYMMETRIC LEAVES2* gene of *Arabidopsis thaliana* regulates formation of a symmetric lamina, establishment of venation and repression of meristem-related homeobox genes in leaves. Development **128:** 1771–1783

Serrano-Cartagena J, Candela H, Robles P, Ponce MR, Pérez-Pérez JM, Piqueras P, Micol JL (2000) Genetic analysis of *incurvata* mutants reveals three independent genetic operations at work in Arabidopsis leaf morphogenesis. Genetics **156:** 1363–1377

Serrano-Cartagena J, Robles P, Ponce MR, Micol JL (1999) Genetic analysis of leaf form mutants from the Arabidopsis Information Service collection. Mol Gen Genet **261:** 725–739

Siegfried KR, Eshed Y, Baum SF, Otsuga D, Drews GN, Bowman JL (1999) Members of the YABBY gene family specify abaxial cell fate in Arabidopsis. Development **126:** 4117–4128

Smyth DR, Bowman JL, Meyerowitz EM (1990) Early flower development in Arabidopsis. Plant Cell **2:** 755–767

Sussex IM (1954) Experiments on the cause of dorsiventrality in leaves. Nature **174:** 351–352

Telfer A, Poethig RS (1998) *HASTY*: a gene that regulates the timing of shoot maturation in *Arabidopsis thaliana*. Development **125:** 1889–1898

Villanueva JM, Broadhvest J, Hauser BA, Meister RJ, Schneitz K, Gasser CS (1999) *INNER NO OUTER* regulates abaxial-adaxial patterning in Arabidopsis ovules. Genes Dev **13:** 3160–3169

Waites R, Hudson A (1995) *phantastica*: a gene required for dorsoventrality in leaves of *Antirrhinum majus*. Development **121:** 2143–2154

Weigel D, Glazebrook J (2002) Arabidopsis: A Laboratory Manual. Cold Spring Harbor Laboratory Press, Cold Spring Harbor, NY, pp 19–39

Williams L, Grigg SP, Xie M, Christensen S, Fletcher JC (2005) Regulation of Arabidopsis shoot apical meristem and lateral organ formation by microRNA *miR166g* and its *AtHD-Zip* target genes. Development **132:** 3657–3668

Yi R, Qin Y, Macara IG, Cullen BR (2003) Exportin-5 mediates the nuclear export of pre-microRNAs and short hairpin RNAs. Genes Dev **17:** 3011–3016

Zhong R, Taylor JJ, Ye ZH (1999) Transformation of the collateral vascular bundles into amphivasal vascular bundles in an Arabidopsis mutant. Plant Physiol **120:** 53–64

Zhong R, Ye ZH (1999) *IFL1*, a gene regulating interfascicular fiber differentiation in Arabidopsis, encodes a homeodomain-leucine zipper protein. Plant Cell **11:** 2139–2152

Zhong R, Ye ZH (2004) *amphivasal vascular bundle 1*, a gain-of-function mutation of the *IFL1/REV* gene, is associated with alterations in the polarity of leaves, stems and carpels. Plant Cell Physiol **45:** 369–385